

# Adaptations of Trabecular Bone to Low Magnitude Vibrations Result in More Uniform Stress and Strain Under Load

STEFAN JUDEX,<sup>1</sup> STEVE BOYD,<sup>2</sup> YI-XIAN QIN,<sup>1</sup> SIMON TURNER,<sup>3</sup> KENNY YE,<sup>4</sup> RALPH MÜLLER,<sup>2</sup>  
AND CLINTON RUBIN<sup>1</sup>

<sup>1</sup>Department of Biomedical Engineering, State University of New York at Stony Brook, Stony Brook, NY; <sup>2</sup>Institute for Biomedical Engineering, Swiss Federal Institute of Technology (ETH) and University Zürich, Zürich, Switzerland; <sup>3</sup>Department of Clinical Sciences, Colorado State University, Ft. Collins, CO; and <sup>4</sup>Department of Applied Mathematics and Statistics, State University of New York at Stony Brook, Stony Brook, NY

(Received 14 November 2001; accepted 8 November 2002)

**Abstract**—Extremely low magnitude mechanical stimuli (<10 microstrain) induced at high frequencies are anabolic to trabecular bone. Here, we used finite element (FE) modeling to investigate the mechanical implications of a one year mechanical intervention. Adult female sheep stood with their hindlimbs either on a vibrating plate (30 Hz, 0.3 g) for 20 min/d, 5 d/wk or on an inactive plate. Microcomputed tomography data of 1 cm bone cubes extracted from the medial femoral condyles were transformed into FE meshes. Simulated compressive loads applied to the trabecular meshes in the three orthogonal directions indicated that the low level mechanical intervention significantly increased the apparent trabecular tissue stiffness of the femoral condyle in the longitudinal (+17%,  $p < 0.02$ ), anterior–posterior (+29%,  $p < 0.01$ ), and medial–lateral (+37%,  $p < 0.01$ ) direction, thus reducing apparent strain magnitudes for a given applied load. For a given apparent input strain (or stress), the resultant stresses and strains within trabeculae were more uniformly distributed in the off-axis loading directions in cubes of mechanically loaded sheep. These data suggest that trabecular bone responds to low level mechanical loads with intricate adaptations beyond a simple reduction in apparent strain magnitude, producing a structure that is stiffer and less prone to fracture for a given load. © 2003 Biomedical Engineering Society. [DOI: 10.1114/1.1535414]

**Keywords**—Bone adaptation, Mechanical stimuli, Mechanical strain and stress, Mechanical properties, Finite element modeling, Bone formation, Osteoporosis, Noninvasive.

## INTRODUCTION

Mechanical parameters believed to guide bones' adaptive process to mechanical stimuli, such as strain magnitude,<sup>16,25</sup> strain rate,<sup>10,19</sup> strain energy density,<sup>3</sup> or strain gradients,<sup>4,9</sup> have been associated with large magnitude mechanical signals. More recently, however, we have shown that extremely small magnitude mechanical

stimuli, inducing strains of less than 10 microstrain ( $\mu\epsilon$ ) in the bone matrix, will increase bone formation when applied at high frequencies (>20 Hz).<sup>21,24</sup> In contrast to many high-impact physical exercise interventions that are unsuitable for patients with fragile bones, the clinical potential of these high-frequency mechanical stimuli to treat and prevent osteoporosis is promising because of their extremely small magnitudes. For any anabolic intervention to be relevant to the clinic, however, it is important to demonstrate its ability to improve the mechanical outcome of the treatment, as it has been learned that an increase in bone quantity does not necessarily lead to a mechanically more competent bone structure.<sup>20,28</sup> Using mechanical compression tests, we have recently verified that a one-year mechanical intervention involving a low magnitude mechanical stimulus, applied for 20 min per day, will increase trabecular bone stiffness in the femoral condyles of sheep.<sup>23</sup> The mechanism by which the bone achieved this increase in stiffness, however, was not immediately clear.

In the study reported here, we used finite element (FE) modeling to more completely characterize the manner in which morphological adaptations of trabecular bone to mechanical vibration influence the resultant strain and stress environment of the trabeculae under load. Specifically, we tested whether simulated FE testing of trabecular bone cubes from vibrated and control animals produces similar increases in apparent stiffness as previously collected from mechanical testing and asked how strain and stress magnitudes within the trabeculae are affected by the adaptations of bone volume and architecture.

## MATERIALS AND METHODS

### *Experimental Design*

Adult female sheep (Warhill, intact ewes, 60–80 kg), 6–8 years of age, were randomized into experimental

Address correspondence to Stefan Judex, Ph.D., Department of Biomedical Engineering, Psychology A Building, State University of New York at Stony Brook, Stony Brook, NY 11794-2580. Electronic mail: stefan.judex@sunysb.edu

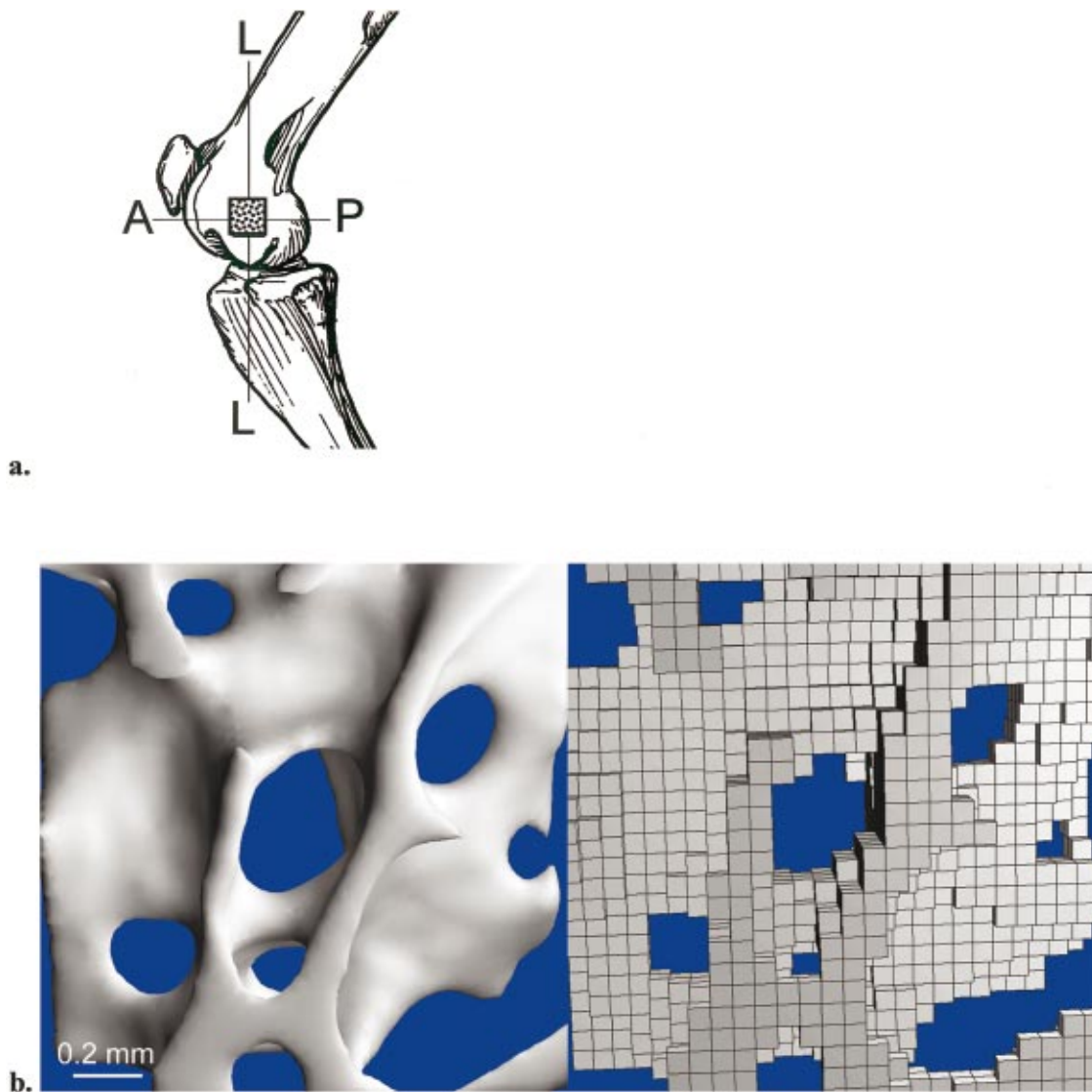


**FIGURE 1.** (a) Trabecular bone cubes were harvested from the medial condyle with careful considerations of the anatomy. A = anterior, P = posterior, L = longitudinal. (b) Direct conversion of  $\mu$ CT data from a central region of the  $(8.7 \text{ mm})^3$  trabecular bone cube to a finite element mesh ( $68 \mu\text{m}$  mesh size).

and age-matched control animals ( $n=9$ , each). Experimental sheep stood with their hind limbs on a vibrating plate oscillating at 30 Hz with peak accelerations of 0.3 g ( $1 \text{ g} = 9.8 \text{ ms}^{-2}$ ), for 20 min per day, five days per week. For the remaining time of the day, experimental animals (like their age-matched controls) were allowed to freely roam a pasture area. Following a one-year experimental intervention, the animals were euthanized by an overdose of a saturated barbiturate and the femora were harvested. Using a water-cooled diamond wafer saw, a 1 cm cube was cut from the medial condyle of the left femur with the longitudinal axis of the femur forming a  $45^\circ$  angle with the longitudinal faces of bone cube [Fig. 1(a)]. The location of the cube within the condyle was primarily determined by the limited amount of tra-

becular bone available to harvest a 1 cm cubed specimen of bone. In the case of excess trabecular bone, the cube was centered within the medial condyle. The experimental design of this study is reported in more detail elsewhere.<sup>22,23</sup> All procedures were reviewed and approved by both the Stony Brook University and Colorado State University animal care committees.

#### *Finite Element Modeling*

Each bone cube was scanned in a microcomputed tomography scanner ( $\mu$ CT 20, Scanco Medical, Switzerland) at a nominal isotropic resolution of  $34 \mu\text{m}$ <sup>26</sup> and filtered and globally thresholded to accurately reconstruct the trabecular microarchitecture [Fig. 1(b)].<sup>17</sup> A volume

of interest was chosen ( $8.7 \times 8.7 \times 8.7 \text{ mm}^3$ ) to reduce boundary artifacts. To limit the computational requirements of the FE analyses, the  $\mu\text{CT}$  voxel data were resampled at an isotropic size of  $68 \mu\text{m}$  prior to converting the three-dimensional bone volume directly into hexahedron-based FE meshes<sup>29</sup> using previously published code<sup>1</sup> [Fig. 1(b)]. This voxel size was the highest resolution available within the limits of the computational resources available (Cray supercomputer). The mesh fractal number<sup>30</sup> ( $f$ ) was calculated for each bone cube to ensure a general adequacy of the FE mesh resolution;  $f = \ln(8 * \text{number of elements} * \text{number of nodes}) / \ln(2)$ . For our specimens, the mean of mesh fractal numbers was 2.52 (range: 2.40–2.63) falling above the recommended minimal mesh fractal number of 1.83 for a rod-like architecture and 2.42 for a plate-like architecture (the maximal mesh fractal number is 3.0 for a hexahedron model). Although a fractal number above the recommended minimal values does not guarantee a 100% accuracy, particularly at the microstructural level, it indicates a reasonable mesh resolution given the computational constraints.

FE analyses simulated axial compression tests of each trabecular bone cube in three orthogonal directions; longitudinal, medial–lateral, and anterior–posterior. A fixed displacement boundary condition was chosen, resulting in perfect axial compression; all nodes at the bone–platen interface were constrained in the plane of the platen. This boundary condition was chosen to mimic the boundary conditions that occurred during mechanical testing of the bone cubes as friction at the platen–bone interface was high for our setup. To test for the effect of this assumption, we compared the magnitudes of the elastic modulus of all trabecular bone cubes (in the longitudinal direction) between fully constrained and unconstrained boundary conditions.

Mechanical testing of the specimens was simulated under displacement control of the platens to mimic mechanical testing conditions. Bone material properties were assumed to be homogeneous and isotropic with a tissue elastic modulus of 5 GPa and a Poisson's ratio of 0.3. An arbitrary displacement of 1% strain was applied to the top platen. The apparent elastic modulus of the bone cubes,  $E$ , was calculated as  $E = F / (A \cdot \epsilon)$  where  $F$  is the reaction force at the bone–platen interface due to the applied strain level,  $A$  is the total surface area of the bone–platen interface, and  $\epsilon$  is the applied 0.01 strain (1%).

To determine the effect of altered bone quantity and microarchitecture (e.g., connectedness) on strain and stress magnitudes of elements within the trabecular bone cube, the strain and stress state including normal and shear components for the three anatomical directions were calculated in each of the approximately one million

finite elements per bone sample. To simplify further analysis, the number of strain and stress data points was limited to 10,000 per bone cube each by re-sampling each data set at a constant interval (i.e., a strain or stress histogram for a given group of sheep contained [number of animals  $\times$  10,000] data points consisted of a total of 70,000 data points for control sheep and 80,000 data points for experimental sheep. This representative data subset was used to determine skewness in the strain and stress distributions of control and experimental trabecular bone cubes as well as for calculating mean stress levels in the bone cubes by averaging the absolute values of all elements (i.e., no distinction was made between tensile and compressive stresses).

Calculations of anisotropy levels of the bone cubes were derived from trabecular structural data as well as from simulated mechanical tests. Structural anisotropy based on  $\mu\text{CT}$  data was computed by mean intercept lengths (MIL),<sup>6</sup> while mechanical anisotropy based on FE data was computed as the ratio of the smallest and largest elastic modulus ( $E$ ) in two orthogonal directions. Because of the arbitrarily chosen magnitudes for the tissue elastic modulus and the strain applied to the bone cubes, strain element data were normalized to the applied apparent strains and tissue stresses were normalized with the applied apparent stress as referent. To calculate the apparent stress, the bone area at the interface with top and bottom platen was averaged. Thus, the presented strain distributions reflected the response of the tissue elements to a given apparent strain while the stress distributions reflected the response to a given apparent stress. For both strain and stress distributions, the magnitude of the arbitrary tissue elastic modulus and the magnitude of the applied (apparent) strain had no effect on the normalized output data because of the linearity of the FE model.

### Statistics

The differences in mechanical properties as well as skewness of microstructural strain and stress distributions, between control, and experimental sheep cubes were evaluated with one-tailed  $t$  tests. One-tailed  $t$  tests were chosen over two-tailed  $t$  tests as, based on previous data on the anabolic nature of low-level mechanical stimuli, the hypothesis of this study was that applied vibrations *enhance* mechanical properties. A single-factor analysis of variance (ANOVA) followed by a Tukey *post hoc* test was used to compare mechanical properties between the three loading directions. Coefficients of determination ( $r^2$ ) determined the correlations between structural and mechanical indices. Data analysis was performed in the statistical software package SPSS for Windows 9.0. The significance level was 0.05 and all data were presented as mean  $\pm$ SD.

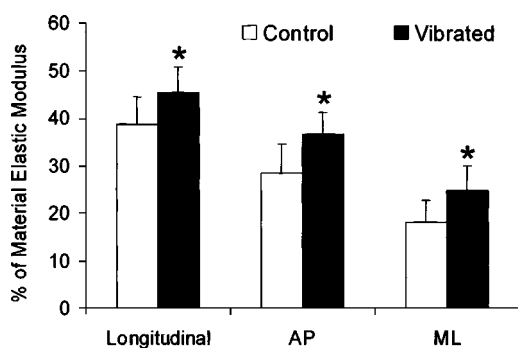


**FIGURE 2.** Apparent elastic tissue modulus expressed as percentage of the arbitrarily chosen tissue elastic modulus for control and vibrated sheep in the three loading directions (mean+SD). Statistically significant differences between experimental and control moduli are denoted by asterisks. AP = anterior–posterior direction; ML = medial–lateral direction.

## RESULTS

During the course of the experiment, one experimental sheep died for reasons unrelated to the mechanical loading protocol and two trabecular bone cubes from control sheep were eliminated from the analyses in this study due to technical difficulties associated with the precision required for cutting the cubes for mechanical testing. The trabecular bone cubes used for FE modeling were identical to the ones subject to mechanical testing in a recent study.<sup>23</sup> The structural three-dimensional  $\mu$ CT data have been reported elsewhere.<sup>23</sup> For the animals used in this study, micro-CT determined trabecular bone volume (BV/TV) of femoral bone cubes was 15% ( $p < 0.02$ ) greater in mechanically stimulated sheep relative to control sheep.

Simulated mechanical compression tests using finite element modeling revealed a strong anisotropy between the three orthogonal directions within the control trabecular bone cubes. Compared to the apparent stiffness in the medial–lateral direction, trabecular bone cubes of control sheep were 57% ( $p < 0.007$ ) stiffer in the anterior–posterior direction and 114% ( $p < 0.001$ ) stiffer in the longitudinal direction (Fig. 2). Low level mechanical vibration for 20 min/d caused a significantly greater apparent trabecular stiffness in all three loading directions. The apparent trabecular elastic modulus in vibrated sheep was 17% larger in the longitudinal direction ( $p < 0.02$ ), 29% larger in the anterior–posterior direction ( $p < 0.01$ ), and 37% larger in the medial–lateral direction ( $p < 0.01$ ) (Fig. 2). Comparing the longitudinal elastic moduli between constrained and unconstrained boundary conditions, we found that the absolute values of the elastic modulus were 5.1% higher under unconstrained condition in both the control and the experimental group. The relative difference in the elastic modulus between control and experimental bone cubes, however,

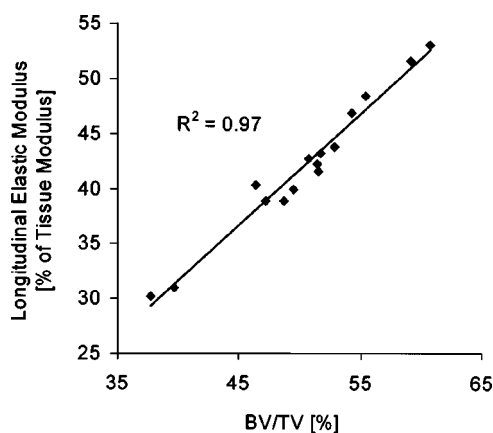


**FIGURE 3.** Correlation between bone volume fraction (BV/TV) of each trabecular cube and its longitudinal elastic apparent modulus from FE expressed as percentage of the arbitrary tissue modulus.

was identical (17.4%) for both boundary conditions. Because of the inverse proportional relation between changes in the elastic modulus and changes in strain magnitude for an applied stress, the larger elastic modulus of experimental bone cubes would cause a reduction in apparent strain magnitude for any given load by 15%, 22%, and 27%, in the longitudinal, anterior–posterior, and medial–lateral direction, respectively.

The elastic moduli obtained previously from a mechanical testing protocol<sup>23</sup> were moderately correlated with elastic moduli calculated by FE testing in the longitudinal direction ( $r^2 = 0.56$ ) but only poor correlations were found in the anterior–posterior ( $r^2 = 0.35$ ) and medial–lateral direction ( $r^2 = 0.01$ ). When correlations were performed separately for data from control and mechanically stimulated sheep, the coefficient of determination significantly increased for control samples in the medial–lateral direction. For all directions,  $r^2$  values for control vs. experimental were: 0.57 vs. 0.33 (longitudinal), 0.33 vs. 0.44 (anterior–posterior), 0.64 vs. 0.13 (medial–lateral).

The elastic modulus obtained from FE loading for each bone cube (control and experimental) in the longitudinal (weightbearing) loading direction was highly correlated with trabecular bone volume fraction ( $r^2 = 0.97$ , Fig. 3) as well as trabecular bone pattern factor,<sup>5</sup> a measure of connectedness ( $r^2 = 0.90$ ) that was 37% larger in experimental than in control cubes. Furthermore, there were moderately high correlations between the structural anisotropy determined by MIL and the mechanical anisotropy that was determined by the ratios of the elastic modulus from FE analyses in the three anatomical directions ( $r^2 = 0.64$ – $0.71$ , Fig. 4).

To test whether the adaptation of the trabecular bone structure to the high-frequency mechanical signal in-

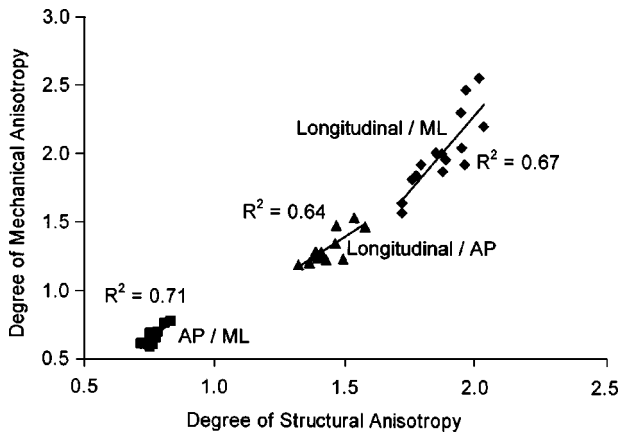


**FIGURE 4.** Correlation between the structural and mechanical anisotropy. Anisotropies were calculated as ratios of MIL (structural) and elastic moduli (mechanical) between the longitudinal and medial–lateral direction (longitudinal/ML), the longitudinal and anterior–posterior direction (longitudinal/AP), and the anterior–posterior and medial–lateral direction (AP/ML).

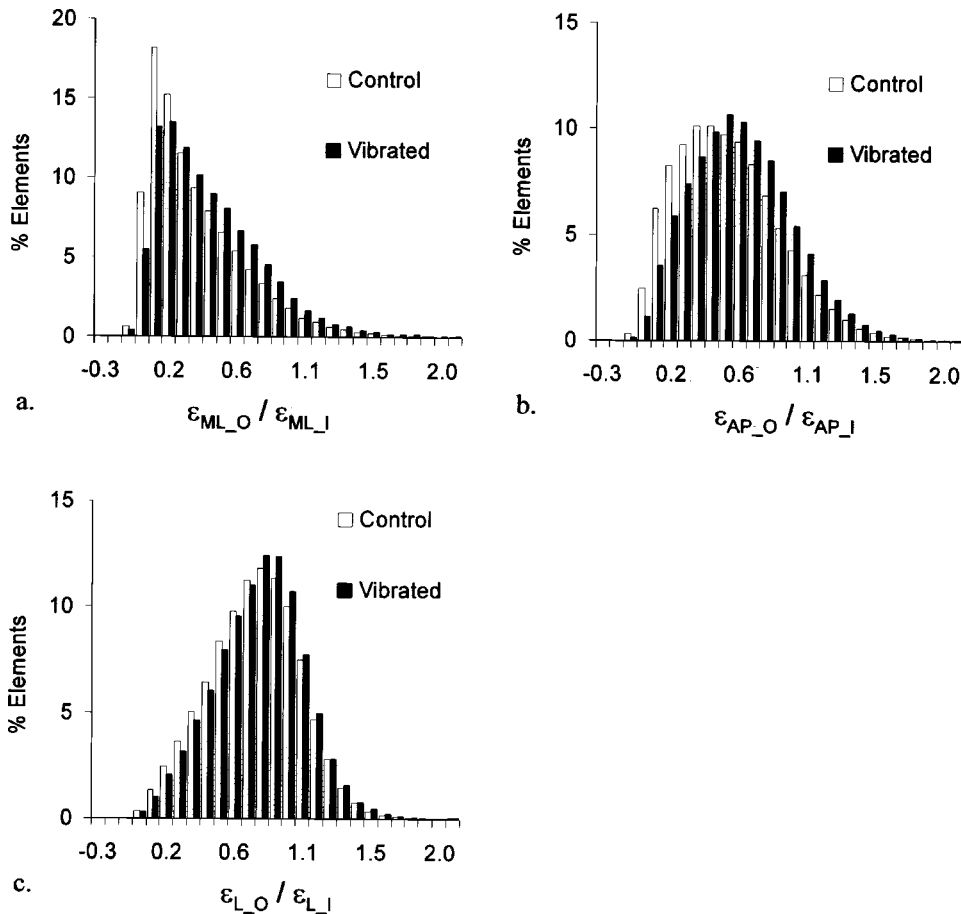


**FIGURE 5.** Histogram displaying the average percentage of elements subject to a range of normal strain magnitudes in the loading direction when control and experimental bone cubes were loaded at a given arbitrary input strain magnitude. Normal strain magnitudes generated within the bone elements ( $\epsilon_0$ ) were normalized to the input apparent strain magnitude ( $\epsilon_i$ ) to eliminate the dependency of the results on the applied strain magnitude. Elements with a value of 1.0 are subject to the apparent strain magnitude. All cubes were strained in the (a) medial–lateral (ML); (b) anterior–posterior (AP); and (c) longitudinal (L) direction.

involved changes beyond a reduction in apparent strain magnitude to a given *load*, the control and experimental bone cubes were subject to a given apparent *strain* magnitude. During this loading, less than 19% of all bone elements experienced strain magnitudes that were greater than the apparent input strain, independent of the applied loading direction or experimental group (Fig. 5). In all three loading directions, application of the same apparent strain magnitude to all cubes led to strains *within* the cubes that were more evenly distributed throughout the elements of trabeculae in experimental bone cubes (Fig. 5); there were fewer elements in cubes harvested from mechanically stimulated animals that were subject to extremely low normal strain magnitudes and more elements that were subject to intermediate strain levels. Quantitatively, the adaptations in bone morphology reduced skewness in the microstructural strain distributions (histograms) of vibrated bone cubes by 14% ( $p < 0.04$ ) in the medial–lateral (ML) and by 24% ( $p < 0.008$ ) in the

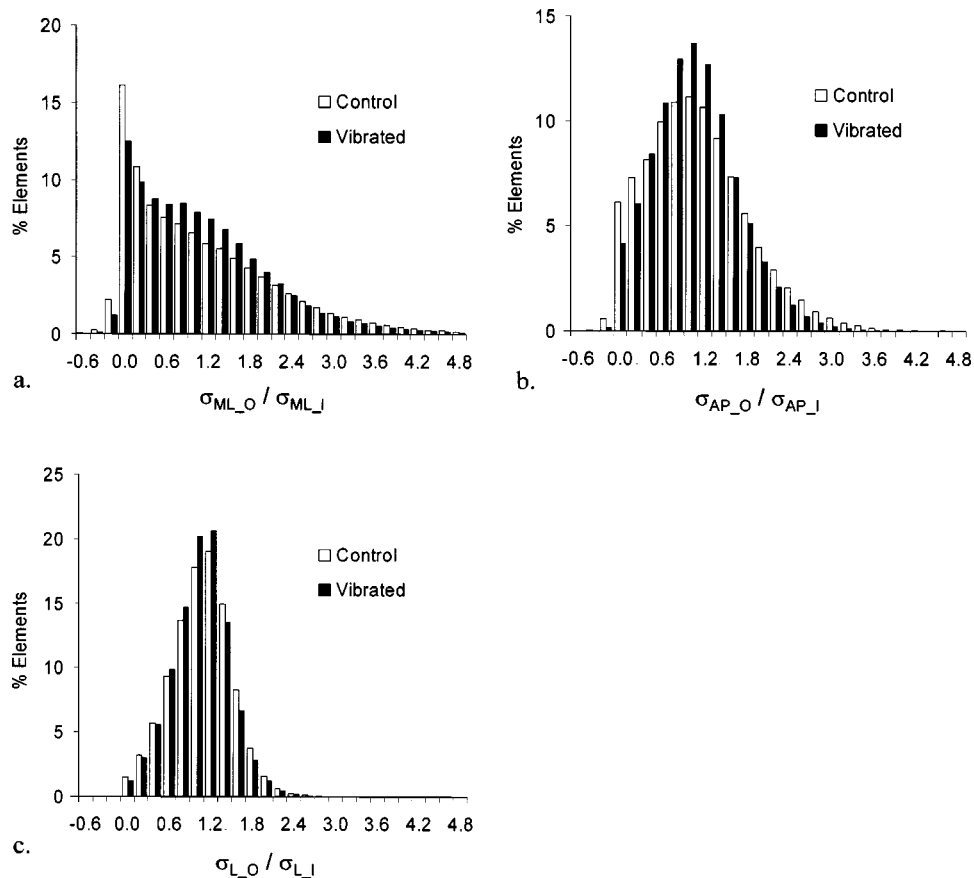


**FIGURE 6.** Difference in stress distributions of loaded trabecular bone cubes from either control or experimental sheep. As stress magnitudes generated within the bone elements ( $\sigma_0$ ) were normalized to the input apparent stress magnitude ( $\sigma_1$ ), output data are the equivalent stress responses in the tissue elements to a given applied stress rather than a given strain (as in Fig. 5). All cubes were loaded in the (a) medial–lateral (ML); (b) anterior–posterior (AP); and (c) longitudinal (L) direction.

anterior–posterior (AP) direction while the strain distributions of both control and experimental sheep were highly symmetrical in the longitudinal (L) direction (see Fig. 7).

When normal stresses generated in the elements were normalized to the apparent stress magnitude (thus simulating the response of the trabecular structure to an applied apparent stress magnitude rather than an apparent strain magnitude), peak stress levels within trabeculae of vibrated bone cubes were decreased and more elements experienced intermediate rather than very high or very low stresses (Fig. 6). Similar to the shift in strain distributions responding to a given apparent strain input, the skewness of the stress distributions in response to a given stress was reduced in vibrated bone cubes in ML (14%,  $p < 0.04$ ) and AP (24%,  $p < 0.009$ ) directions but not in the L direction (Fig. 7). When averaged across all elements, stress magnitudes in bone cubes from vibrated sheep compared to controls were smaller by 1%, 5%, and 3% (ML, AP, L). The average stress magnitude of the 10% of elements that were stressed the most within the trabecular structure, was 11% (ML), 13% (AP), and

4% (L) smaller in trabeculae that were subjected to the low level mechanical stimulus.

Peak shear strain and stress magnitudes in individual trabeculae were negligible compared to normal strain (stress) magnitudes and the differences in the distributions between control and experimental bone cubes were smaller.

## DISCUSSION

This study provided a demonstration of how tissue strains and stresses are affected by the adaptation of trabecular bone to very low magnitude, high frequency mechanical signals. Simulated compressive loads were applied to cubes harvested from the medial femoral condyle and finite element analyses evaluated the apparent and microstructural outcome of a one-year mechanical intervention using these mechanical stimuli. As compared to control bones, 20 min of mechanical loading per day significantly increased apparent stiffness in all three anatomical directions and reduced peak stresses (and strains) generated within trabeculae for a given compressive

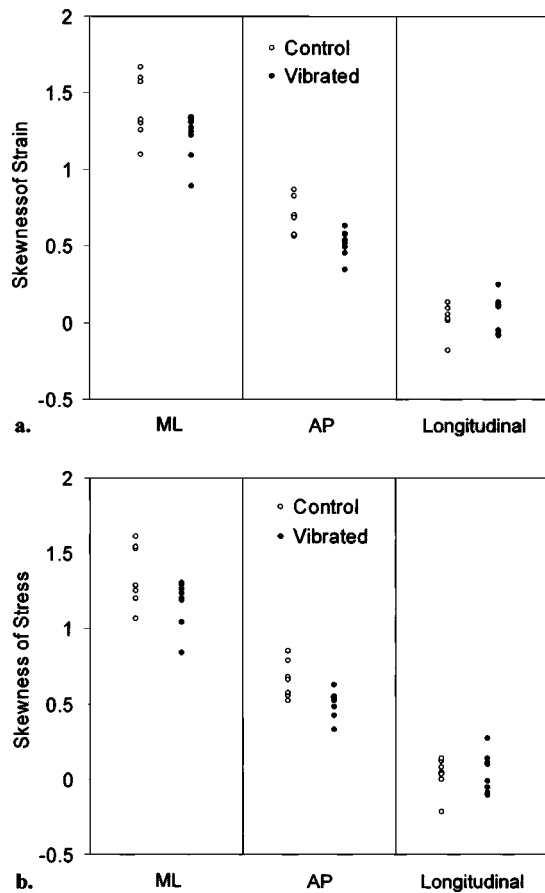


**FIGURE 7. Skewness values for normal (a) strain and (b) stress distributions derived from all control and vibrated trabecular bone cubes in the three orthogonal directions. Mean skewness values were significantly smaller in vibrated bone cubes in both the medial–lateral (ML) and anterior–posterior (AP) and direction.**

sive load. Furthermore, bone remodeling in response to the mechanical loading regime induced adaptations that went beyond reducing peak stress magnitudes in off-axis loading directions with more elements assuming intermediate (rather than low or high) strains and stresses across trabeculae.

For the simulated loading of the finite element meshes, we did not attempt to replicate the *in vivo* loading conditions during habitual loading but used simple axial compression tests instead that allowed us to differentiate the adaptive response between the three orthogonal directions of the bone cubes. The largest differences in trabecular bone stiffness between control and mechanically stimulated sheep occurred in the two directions, ostensibly experiencing lower levels of high-frequency mechanical stimulation than the longitudinal direction, thus making the bone structure preferentially stiffer in off-axis directions. The only  $\mu$ CT parameter that was capable of distinguishing structural changes in the three directions, mean intercept length (MIL), was

unable to directly account for this phenomenon as MIL was decreased by 8.3% ( $p < 0.03$ ) in the longitudinal direction and by 3.3% ( $p = 0.2$ ) and 4.1% ( $p < 0.02$ ) in the anterior–posterior and medial–lateral direction. Given the complex relation between trabecular architecture and its directional stiffness, the inability of MIL to predict changes in stiffness is little surprising and demonstrates the need to mechanically assess structural changes of bone’s adaptive response for a comprehensive intervention outcome evaluation.

While the smaller increase in bone stiffness in the weight-bearing direction is counterintuitive from an engineering perspective, the mechanical adaptations in off-axis directions may be particularly beneficial for reducing the risk of fracture as the direction of forces leading to fractures (e.g., during falling) also does not tend to coincide with the direction of habitual loading events. Furthermore, a preferential off-axis increase in bone stiffness would be consistent with a growing body of evidence that the primary goal of the adaptation of bone to mechanical stimuli is not a reduction in peak strain magnitude during habitual loading and that bone is sensitive to other components of its mechanical environment.<sup>4,9,10,15,19,27</sup>

The adaptations in off-axis directions also became apparent by comparing strain distributions (histograms) between control and vibrated animals as bone strain and stress histograms were more symmetrical in vibrated sheep except for the longitudinal direction in which strain (stress) data from control sheep were already symmetrically distributed. These data suggest that trabecular bone adapts to mechanical loading with site-specific additions of bone tissue that causes bone strain distributions to become more uniform in distribution (i.e., strain magnitudes in trabecular elements take on predominantly intermediate values in a relative sense). This goal of achieving more uniform strain distributions during the adaptive process is supported by the observation that stress and strain histograms were the least skewed in the predominant direction of habitual mechanical loading (longitudinal) and displayed the greatest skewness in the direction that experiences the least amount of loading during functional activities (medial–lateral). While a mechanosensory mechanism for such a relationship is yet to be elucidated, it is interesting to note that strain gradients, which have previously been suggested to guide the adaptive process in cortical and trabecular bone,<sup>4,9,27</sup> would be reduced in such a realignment of strain distributions.

No experimental variation is introduced by converting  $\mu$ CT voxels to finite element meshes and accurate meshes can be obtained at relatively low resolutions.<sup>8,18</sup> On the other hand, large variations may be associated with mechanical testing itself<sup>13</sup> as well as with storage procedures of the specimens.<sup>2</sup> Nevertheless, previous

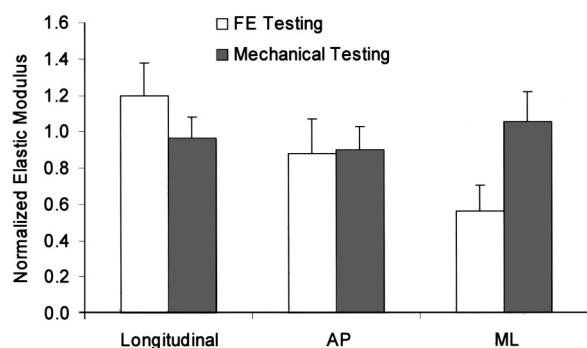


**FIGURE 8.** Comparison of apparent elastic trabecular moduli from control sheep demonstrating a high degree of directionality for data from FE testing but not from mechanical testing. For each testing procedure and direction, all data points were normalized to the combined average apparent modulus in the three directions.

studies found high correlations between experimentally determined mechanical properties of trabecular bone specimens and values computed by simulated FE testing.<sup>7,11,14</sup> Samples of our control group showed moderately high correlation coefficients between stiffness data collected previously from mechanical compression testing<sup>23</sup> and our current stiffness data from simulated FE testing. Correlations for vibrated sheep cubes, at least in the longitudinal and medial–lateral direction, were lower. The absolute magnitude of the tissue elastic modulus (input variable for FE analyses) had no direct effect on the relative differences between treatment groups because all output data from FE models were normalized to the input variable and the same elastic modulus was assumed for control and experimental bones.

Conceivably, the mechanical intervention nonuniformly altered the tissue elastic modulus between and within experimental animals although histomorphometric data indicated that remodeling activity in control as well as in mechanically stimulated sheep was relatively low.<sup>22</sup> It is more likely, however, that the mechanical testing procedure used previously was not sufficiently sensitive to detect altered stiffness values of experimental bone cubes in off-axis loading directions, rather than an incorrect assumption of tissue homogeneity accounting for the differential results. While the elastic moduli in the three orthogonal directions obtained from simulated FE testing exhibited, as expected,<sup>12</sup> a high degree of directionality, trabecular bone cubes that were subjected to mechanical testing did not display any degree of mechanical anisotropy (Fig. 8). Furthermore, and in contrast to the mechanical testing data, the magnitude of the three elastic moduli from each bone cube (both control and experimental) as determined by FE testing was ranked in a consistent order from longitudinal (highest) to medial–lateral (lowest). Nevertheless, further studies that may include the microstructural assessment of bone material

properties (e.g., nanoindentation) will be necessary to explain the discrepancies observed between our two studies.

In summary, we found that altered trabecular bone quantity and microarchitecture induced by low level mechanical vibration produced large nonuniform increases in mechanical stiffness in the three orthogonal directions and decreased strain and stress levels throughout individual trabeculae for a given applied load. The morphological trabecular changes reduced skewness in the distributions of stress and strain, perhaps a goal of the adaptive process of trabecular bone to increased mechanical loading. Taking together, these adaptations may effectively protect the skeleton particularly from large off-axis loading events and lead to reduced fracture rates, the ultimate measure of any anabolic treatment with clinical potential.

## ACKNOWLEDGMENTS

The authors are grateful to the National Institute of Health (AR.43498), the Alberta Heritage Foundation for Medical Research (Canada), and the Natural Sciences and Engineering Research Council of Canada for funding of this work.

## REFERENCES

- Boyd, S. K., R. Muller, and R. F. Zernicke. Mechanical and architectural bone adaptation in early stage experimental osteoarthritis. *J. Bone Miner. Res.* 17:687–694, 2002.
- Callaghan, J. P., and S. M. McGill. Frozen storage increases the ultimate compressive load of porcine vertebrae. *J. Orthop. Res.* 13:809–812, 1995.
- Fyhrie, D. P., and D. R. Carter. A unifying principle relating stress to trabecular bone morphology. *J. Orthop. Res.* 4:304–317, 1986.
- Gross, T. S., J. L. Edwards, K. J. McLeod, and C. T. Rubin. Strain gradients correlate with sites of periosteal bone formation. *J. Bone Miner. Res.* 12:982–988, 1997.
- Hahn, M., M. Vogel, M. Pompesius-Kempa, and G. Delling. Trabecular bone pattern factor: A new parameter for simple quantification of bone microarchitecture. *Bone (N.Y.)* 13:327–330, 1992.
- Hildebrand, T., A. Laib, R. Muller, J. Dequeker, and P. Rueggsegger. Direct three-dimensional morphometric analysis of human cancellous bone: Microstructural data from spine, femur, iliac crest, and calcaneus. *J. Bone Miner. Res.* 14:1167–1174, 1999.
- Hou, F. J., S. M. Lang, S. J. Hoshaw, D. A. Reimann, and D. P. Fyhrie. Human vertebral body apparent and hard tissue stiffness. *J. Biomech.* 31:1009–1015, 1998.
- Jacobs, C. R., B. R. Davis, C. J. Rieger, J. J. Francis, M. Saad, and D. P. Fyhrie. NACOB presentation to ASB Young Scientist Award: Postdoctoral. The impact of boundary conditions and mesh size on the accuracy of cancellous bone tissue modulus determination using large-scale finite-element modeling. North American Congress on Biomechanics. *J. Biomech.* 32:1159–1164, 1999.



- <sup>9</sup>Judex, S., T. S. Gross, and R. F. Zernicke. Strain gradients correlate with sites of exercise-induced bone-forming surfaces in the adult skeleton. *J. Bone Miner. Res.* 12:1737–1745, 1997.
- <sup>10</sup>Judex, S., and R. F. Zernicke. High-impact exercise and growing bone: Relation between high strain rates and enhanced bone formation. *J. Appl. Physiol.* 88:2183–2191, 2000.
- <sup>11</sup>Kabel, J., B. Van Rietbergen, M. Dalstra, A. Odgaard, and R. Huiskes. The role of an effective isotropic tissue modulus in the elastic properties of cancellous bone. *J. Biomech.* 32:673–680, 1999.
- <sup>12</sup>Keaveny, T. M., and W. C. Hayes. A 20-year perspective on the mechanical properties of trabecular bone. *J. Biomech. Eng.* 115:534–542, 1993.
- <sup>13</sup>Keaveny, T. M., T. P. Pinilla, R. P. Crawford, D. L. Kopperdahl, and A. Lou. Systematic and random errors in compression testing of trabecular bone. *J. Orthop. Res.* 15:101–110, 1997.
- <sup>14</sup>Ladd, A. J., J. H. Kinney, D. L. Haupt, and S. A. Goldstein. Finite-element modeling of trabecular bone: Comparison with mechanical testing and determination of tissue modulus. *J. Orthop. Res.* 16:622–628, 1998.
- <sup>15</sup>Mosley, J. R., and L. E. Lanyon. Strain rate as a controlling influence on adaptive modeling in response to dynamic loading of the ulna in growing male rats. *Bone (N.Y.)* 23:313–318, 1998.
- <sup>16</sup>Mosley, J. R., B. M. March, J. Lynch, and L. E. Lanyon. Strain magnitude related changes in whole bone architecture in growing rats. *Bone (N.Y.)* 20:191–198, 1997.
- <sup>17</sup>Muller, R., H. Van Campenhout, B. Van Damme, G. Van Der Perre, J. Dequeker, T. Hildebrand, and P. Ruegsegger. Morphometric analysis of human bone biopsies: A quantitative structural comparison of histological sections and microcomputed tomography. *Bone (N.Y.)* 23:59–66, 1998.
- <sup>18</sup>Niebur, G. L., J. C. Yuen, A. C. Hsia, and T. M. Keaveny. Convergence behavior of high-resolution finite element models of trabecular bone. *J. Biomech. Eng.* 121:629–635, 1999.
- <sup>19</sup>O'Connor, J. A., L. E. Lanyon, and H. MacFie. The influence of strain rate on adaptive bone remodelling. *J. Biomech.* 15:767–781, 1982.
- <sup>20</sup>Riggs, B. L., S. F. Hodgson, W. M. O'Fallon, E. Y. Chao, H. W. Wahner, J. M. Muhs, S. L. Cedel, and L. J. Melton. Effect of fluoride treatment on the fracture rate in postmenopausal women with osteoporosis. *N. Engl. J. Med.* 322:802–809, 1990.
- <sup>21</sup>Rubin, C., A. S. Turner, S. Bain, C. Mallinckrodt, and K. McLeod. Anabolism: Low mechanical signals strengthen long bones. *Nature (London)* 412:603–604, 2001.
- <sup>22</sup>Rubin, C., A. S. Turner, C. Mallinckrodt, C. Jerome, K. McLeod, and S. Bain. Mechanical strain, induced noninvasively in the high-frequency domain, is anabolic to cancellous bone, but not cortical bone. *Bone (N.Y.)* 30:445–452, 2002.
- <sup>23</sup>Rubin, C., A. S. Turner, R. Muller, E. Mittra, K. McLeod, W. Lin, and Y. X. Qin. Quantity and quality of trabecular bone in the femur are enhanced by a strongly anabolic, noninvasive mechanical intervention. *J. Bone Miner. Res.* 17:349–357, 2002.
- <sup>24</sup>Rubin, C., G. Xu, and S. Judex. The anabolic activity of bone tissue, suppressed by disuse, is normalized by brief exposure to extremely low-magnitude mechanical stimuli. *FASEB J.* 15:2225–2229, 2001.
- <sup>25</sup>Rubin, C. T., and L. E. Lanyon. Regulation of bone mass by mechanical strain magnitude. *Calcif. Tissue Int.* 37:411–417, 1985.
- <sup>26</sup>Ruegsegger, P., B. Koller, and R. Muller. A microtomographic system for the nondestructive evaluation of bone architecture. *Calcif. Tissue Int.* 58:24–29, 1996.
- <sup>27</sup>Turner, C. H., V. Anne, and R. M. Pidaparti. A uniform strain criterion for trabecular bone adaptation: Do continuum-level strain gradients drive adaptation? *J. Biomech.* 30:555–563, 1997.
- <sup>28</sup>Turner, C. H., I. Owan, E. J. Brizendine, W. Zhang, M. E. Wilson, and A. J. Dunipace. High fluoride intakes cause osteomalacia and diminished bone strength in rats with renal deficiency. *Bone (N.Y.)* 19:595–601, 1996.
- <sup>29</sup>Van Rietbergen, B., H. Weinans, R. Huiskes, and A. Odgaard. A new method to determine trabecular bone elastic properties and loading using micromechanical finite-element models. *J. Biomech.* 28:69–81, 1995.
- <sup>30</sup>Van Rietbergen, B., H. Weinans, B. J. W. Polman, and R. Huiskes. Computational strategies for iterative solutions of large FEM applications employing voxel data. *Int. J. Numer. Methods Eng.* 39:2743–2767, 1996.